https://doi.org/10.5194/egusphere-2026-3979
Preprint. Discussion started: 29 July 2026

Near-absence of surface zooplankton and pervasive anthropogenic particles along a zonal North Atlantic transect: a multi-vessel citizen-science image survey

Howard Dryden[1] and Diane Duncan[1]
[1]GOES Foundation / Seahorse Point Nature Laboratory, Bastimentos, Bocas del Toro, Panama
Correspondence to: Howard Dryden (howard@goesfoundation.com; ORCID 0000-0002-5068-2113)

Abstract

Climate policy treats carbon dioxide as the single lever on the climate. We suggest a second one has been overlooked: the marine biodiversity that builds and maintains the ocean surface microlayer (SML), and that pollution is now degrading. Water vapour, not CO_2, is the largest single contributor to the natural greenhouse effect and the strongest feedback on warming. The ocean supplies most of that vapour across the 71% of the planet it covers, and the thin biogenic lipid-and-surfactant film phytoplankton spread over the sea surface helps govern how readily it evaporates and forms aerosol. That same film gathers lipophilic “forever” chemicals, together with the microplastic and black-carbon soot they cling to, to levels far above the water beneath, where they turn toxic to the plankton that hold the ecosystem together.

An automated image pipeline sized and classified 51,547 particles larger than 20 µm in 352 georeferenced surface samples from eight sailing vessels crossing the trade-wind North Atlantic. Zooplankton were absent from 93.8% of stations. Black carbon appeared at 89.8%, microplastic particles at 69.9%, microfibres at 22.4% and phytoplankton at 81.8%; 99.2% of everything counted measured below 200 µm. A separate 110-image, GPS-tagged crossing returned zero zooplankton at every point on the track, and a plankton net towed at the surface by day and by night confirmed the scarcity directly, returning roughly 0.2 to 0.5 animals per cubic metre — far below any productive ocean. In short, this surface layer is stripped of animal plankton and steeped in combustion and plastic residue. We trace what that may mean for the microlayer, for water-vapour feedback and cloud formation, and for ocean pH, and argue that cutting pollution has to sit beside cutting carbon.

1. Introduction

Every ocean wears a surface microlayer: a distinct skin, somewhere between 1 and 1000 µm thick (Zhang et al., 2003), made of proteins, carbohydrates and lipids from marine plankton and laced with particulate matter, sub-micron and microplastic, black-carbon soot and chelated metals (Garrett, 1967; Williams et al., 1986; Cunliffe et al., 2013). It is not inert. The SML is a living biofilm — bacteria and nanoplankton suspended in a mucopolysaccharide gel with the lipids and surfactants — and it damps turbulence, throttles gas exchange, seeds aerosols and clouds, and slows the escape of water from the sea surface (O’Dowd et al., 1997; Cunliffe et al., 2013).

Water vapour is the largest single contributor to the natural greenhouse effect and the strongest feedback on CO_2-driven warming. Its abundance climbs with temperature, through the Clausius–Clapeyron

https://doi.org/10.5194/egusphere-2026-3979
Preprint. Discussion started: 29 July 2026

relation, but what happens at the air–sea boundary matters too (Held and Soden, 2000). Our proposition is simple: the SML is a second, biologically maintained control on that boundary, plankton keep it in repair, and pollution is wearing it away.

The trade-wind North Atlantic sampled here is an oligotrophic, subtropical-gyre-influenced region crossed by the North Equatorial and Canary currents, where surface productivity is expected to be low. What is poorly known is the standing stock of the smallest surface plankton and the burden of anthropogenic particles in the 20–200 µm range, because conventional oceanography samples mainly from 5–200 m depth and rarely resolves this fraction at the ocean surface. The science question this survey addresses is therefore direct: is the trade-wind Atlantic surface layer depleted of animal plankton and laden with combustion and plastic residue, and if so, what does that imply for the surface microlayer, for water-vapour feedback and cloud formation, and for ocean pH? The answer matters because the physical and biological condition of the sea surface is itself a climate variable that carbon-only models omit.

2. The GOES North Atlantic survey

2.1 Study region, vessels and timing

The survey covers the zonal trade-wind corridor from the Canary Islands and Cape Verde to the Caribbean and Suriname, framed to the east by the West African coast and to the west by the Lesser Antilles and the South American shelf, and shaped by the North Atlantic subtropical gyre, the Canary Current and the North Equatorial Current (Fig. 1). Eight sailing vessels contributed the recoverable photographic archive; each vessel, its route, station count and longitudinal span are listed in Table 3. The crossings were contemporaneous: per-image timestamps exist only for the GPS-tagged Copepod crossing (8 January – 3 February 2022) — the sailing vessel Copepod was skippered by the authors — to which the sampling dates of the other vessels are referenced (Fig. 1). One vessel (Emma) additionally carried out a higher-latitude North Atlantic return leg in May 2023 (Fig. 1); that leg is the only part of the archive outside the trade-wind belt and outside the January–February crossing season.

https://doi.org/10.5194/egusphere-2026-3979
Preprint. Discussion started: 29 July 2026

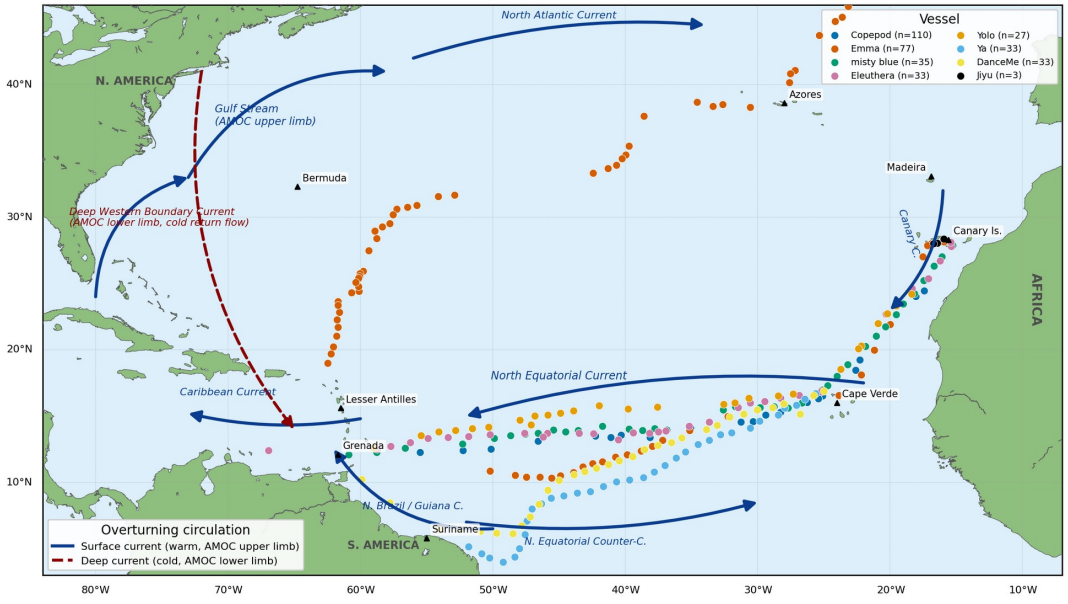

Figure 1. Study region, vessels and circulation. Eight vessels and their stations along the zonal trade-wind crossing from the Canary Islands and Cape Verde to Grenada and Suriname; Madeira, Bermuda and the Lesser Antilles are marked for reference. The trade-wind crossing was sampled between 8 January and 3 February 2022, timing referenced to the GPS-tagged Copepod crossing; the vessel Emma additionally sampled a higher-latitude North Atlantic return leg (to ~50°N) in May 2023. Coastlines © Natural Earth.

2.2 Image-analysis pipeline

Crews drew surface samples on a fixed twice-daily schedule — 12:00 (local noon) and 24:00 (local midnight), so that about half of all samples were collected at night — filtered them to ~20 µm, and photographed the filter paper under a microscope whose maximum magnification places a single 5 mm aperture (5000 µm) across the field of view, giving an imaging resolution of about 20 µm. An automated pipeline (OpenCV) locates the filter aperture, detects every particle larger than 20 µm, measures it against the known 5 mm field width, and classifies it as zooplankton, phytoplankton, plastic particle, plastic fibre or black (combustion) carbon. Each image was tied to a position from its GPS tag or its field-log row. In total the pipeline sized and classified 51,547 particles at 352 georeferenced stations.

2.3 Near-absence of zooplankton

The dominant result is an absence. Zooplankton were not detected at 93.8% of stations, and the entire archive yielded only 44 animal-class objects — the largest things measured (median 328 µm). The absence was not confined to any vessel or region (Fig. 2), and an independent set of 110 GPS-tagged images from the Copepod crossing returned no zooplankton at any point on the track. Because about half of all surface samples were collected at midnight and showed the same near-absence as those taken at midday, the scarcity is not an artefact of daytime diel vertical migration into deeper water; counts

https://doi.org/10.5194/egusphere-2026-3979
Preprint. Discussion started: 29 July 2026

were uniformly so low that the imaging archive was not partitioned by time of day. The stations along any one vessel's track are, moreover, not fully independent — neighbouring samples lie in similar water — but the same near-absence appears independently on all eight vessels' separate routes (Table 3), so it is not a statistical artefact of autocorrelation within a single cruise. Microplastic ingestion and pollutant toxicity can suppress copepods and other grazing zooplankton (Cole et al., 2013; Desforges et al., 2015; Galloway et al., 2017; Botterell et al., 2019; Ma et al., 2020; Pabortsava and Lampitt, 2020); a long-term decline in phytoplankton has also been reported, although its magnitude remains debated (Boyce et al., 2010). An independent surface net-tow survey, by day and by night, confirmed this scarcity directly (Sect. 2.8). Densities of 0.2–0.5 animals m^{-3} lie two to three orders of magnitude below published Atlantic surface values: productive open-ocean and shelf waters typically carry hundreds to thousands of mesozooplankton per cubic metre, and even the oligotrophic subtropical gyres — sampled on the global Malaspina circumnavigation with a coarse 300 µm net that undercounts the smallest copepods — still hold upward of 200 individuals per cubic metre in the epipelagic layer (Woodd-Walker et al., 2000; Vereshchaka et al., 2017; Fernández de Puelles et al., 2019). The surface stock recorded here is therefore of order a thousandfold lower than even the poorest comparable open-ocean waters. The scarcity is therefore a genuine surprise rather than merely the expected low productivity of the trade-wind belt. The result also sits within a wider trend: an integrated long-term assessment of the Northeast Atlantic (Portugal to Norway), which overlaps the higher-latitude return leg of the present survey, reported parallel declines in both phytoplankton biomass and zooplankton abundance over more than six decades, with none of the assessed pelagic habitats achieving "Good" environmental status (McQuatters-Gollop et al., 2026). Our near-total absence of surface animal plankton along the trade-wind belt is consistent with, and extends further south, that broad-scale deterioration of the plankton base.

https://doi.org/10.5194/egusphere-2026-3979
Preprint. Discussion started: 29 July 2026

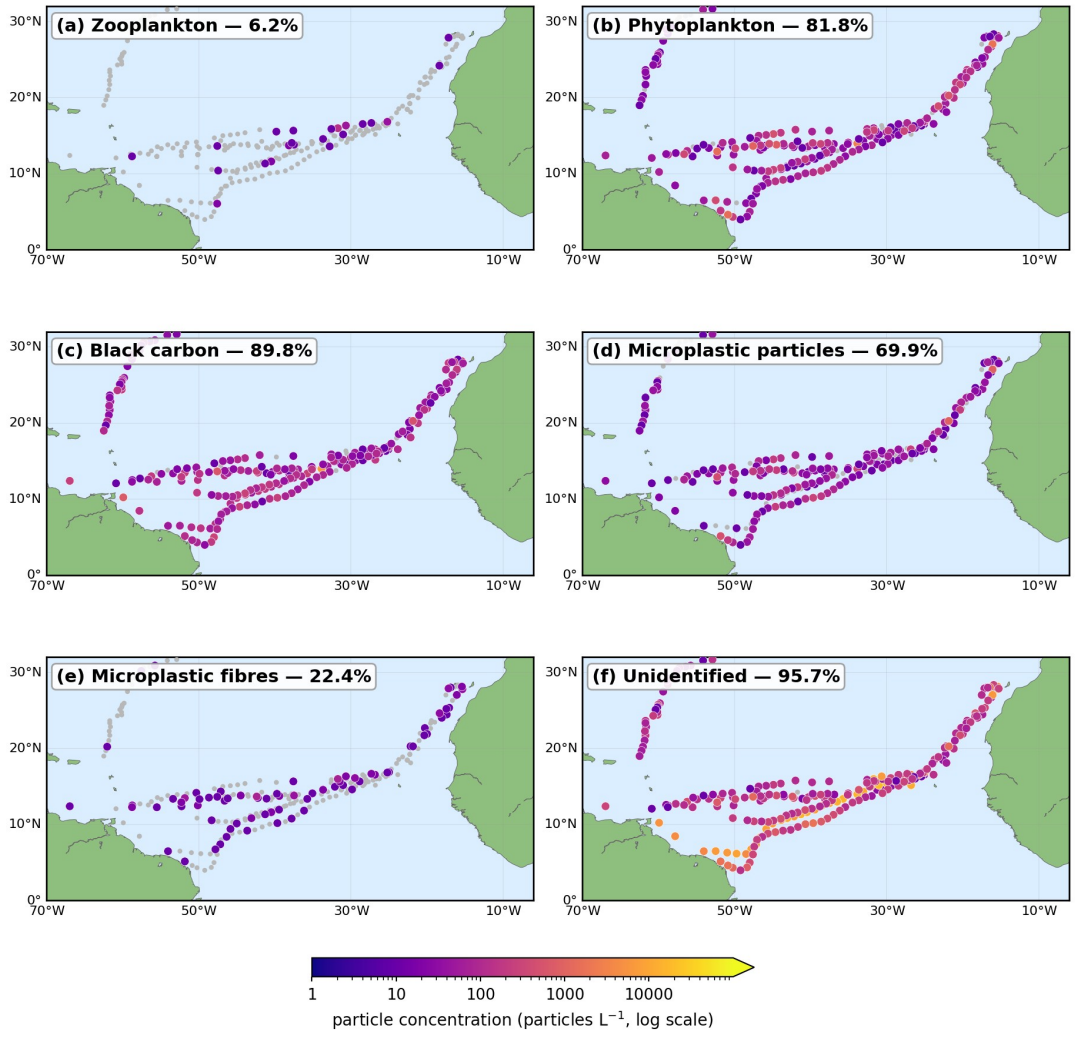

Figure 2. Image-derived particle-class concentrations across the mapped stations (grey = class absent; colour = particles L^{-1} on a logarithmic scale). (a) Zooplankton, present at only 6.2% of stations; (b) phytoplankton (81.8%); (c) black carbon (89.8%); (d) microplastic particles (69.9%); (e) microplastic fibres (22.4%); and (f) unidentified fine material (95.7%). Percentages are the share of all 352 sampled stations at which each class was detected.

2.4 Ubiquitous black carbon and microplastic

Against that empty animal background, anthropogenic particles were near-universal. Black carbon was present at 89.8% of stations (3,559 particles; median 31 µm), microplastic particles at 69.9% and microfibres at 22.4% (median fibre length 204 µm). Phytoplankton-class objects were present at 81.8% of stations. Plastic and black carbon are now documented throughout the open ocean, including the Atlantic water column, the remote marine atmosphere, polar snow, and even the fauna of deep-sea hydrothermal vents more than 2,000 m down (Bond et al., 2013; Cózar et al., 2014; Allen et al., 2019;

5

https://doi.org/10.5194/egusphere-2026-3979
Preprint. Discussion started: 29 July 2026

Bergmann et al., 2019; Pabortsava and Lampitt, 2020; Trainic et al., 2020; Aves et al., 2022; Lee et al., 2026), so the pervasiveness seen here is expected. Expressed as concentrations (Table 1; each station draws a full 0.5-litre sample, filtered through the five Ø5 mm apertures at ~100 mL each, and particles are counted across all five apertures, so the per-litre concentration is the whole-station count × 2 — a full 0.5 L sampled at every station, not a 100 mL grab scaled up), the class loads are strongly right-skewed: median values across the 352 stations were about 12 /L for black carbon, 10 /L for phytoplankton and 5 /L for microplastic particles, with the busiest stations reaching several hundred per litre, while zooplankton stayed at or near zero (median 0; present at only 6.2% of stations). Along the zonal transect the class means showed no strong east–west gradient (Fig. 3); elevated individual loads tended to occur near the continental margins at either end — most notably the Canary and Northwest-African margin in the east, and to a lesser extent the South American shelf in the west — consistent with terrestrial and riverine input (Mai et al., 2020). The otherwise even dispersion of plastic across the open ocean, far from any land source, may itself indicate that a substantial proportion arrives by atmospheric deposition in rainfall rather than by riverine transport alone (Allen et al., 2019; Brahney et al., 2021). Physical setting shapes this pattern: most of the transect crosses the quiescent, oligotrophic interior of the subtropical gyre, but wind-driven coastal upwelling along the Northwest African margin near the Canary Current, and wake-driven mixing downstream of the Canary and Cape Verde islands, can locally enrich near-surface productivity and redistribute buoyant particles, while the trade-wind drift and the North Equatorial Current carry surface material westward toward the Caribbean.

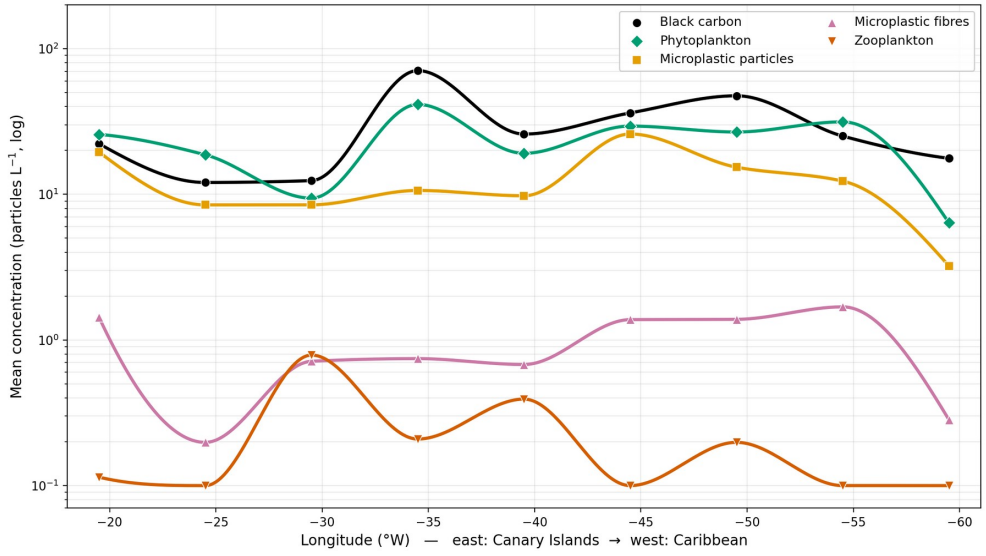

Figure 3. Mean particle-class concentration along the crossing, east (Canary Islands) to west (Caribbean), as smooth curves through longitude-bin means (markers). Zooplankton remain the lowest class across the whole transect; carbon, microplastic and phytoplankton are broadly comparable with no strong longitudinal gradient.

6

https://doi.org/10.5194/egusphere-2026-3979
Preprint. Discussion started: 29 July 2026

2.5 The surface field is overwhelmingly sub-200 µm

The particle field was very small: 99.2% of all classified particles measured below 200 µm, bunched against the 20 µm filtration and imaging limit (Fig. 4). Plastic fibres formed a distinct larger mode (median 204 µm) and the rare zooplankton occupied the >200 µm range. Because abundance is concentrated at the smallest resolvable size, the true particle burden — including the sub-micron fraction that the SML preferentially binds — is certainly higher than these counts, which should be read as a floor.

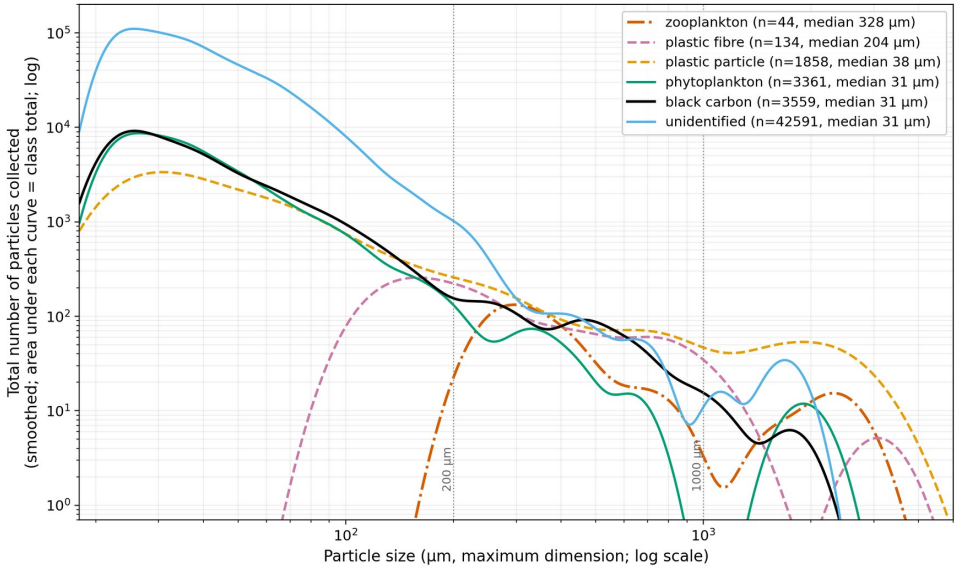

Figure 4. Smoothed particle size distribution by class (log–log). The vertical axis is the total number of particles collected across the whole survey; the area under each class curve equals that class's total count (given as n in the legend). Dashed lines mark 200 and 1000 µm. The unidentified fine fraction dominates near the 20–40 µm limit; plastic fibres and the rare zooplankton form the larger modes.

2.6 Example fields and their contents

To illustrate the material recorded at individual stations, Figure 5 shows three representative filter fields, each from a different station — that is, from a separate 0.5-litre filter sample, not three of the five holes of one filter. At each station the total sample volume is 500 mL, passed through the five Ø5 mm filter holes, so each imaged field represents the particle content of approximately 100 mL of filtered seawater. They span the range encountered: a pigment-rich field with abundant partially combusted carbon and both microplastic fibres and particles; a field containing chain-forming and star-shaped diatoms with a frayed microfibre bundle and scattered carbon; and a near-empty field typical of the majority of stations, at which animal zooplankton were absent. Identifications from the images are tentative — "partially combusted carbon" denotes dark, colourless particles, an optical description that may also include dark

7

https://doi.org/10.5194/egusphere-2026-3979
Preprint. Discussion started: 29 July 2026

plastic or sediment, and the microplastic-versus-phytoplankton assignment for some objects is provisional pending FTIR/Raman confirmation.

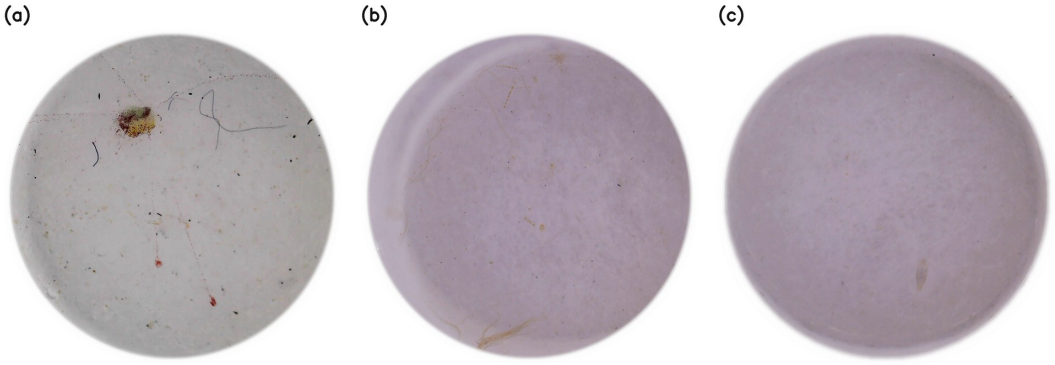

Figure 5. Representative filter fields (white background; faint grey circle marks the 5 mm field boundary). (a) pigmented phytoplankton aggregate with abundant partially combusted carbon and blue and red microplastic fibres and particles; (b) chain-forming and star-shaped diatoms with a frayed microfibre bundle and scattered carbon; (c) a near-empty field with a single probable pennate diatom. Each panel is from a different station (a separate 0.5-litre filter sample), not a different hole of the same filter; each field shows the particle content of approximately 100 mL of filtered seawater.

2.7 Validation and limitations of the classification

We cross-checked the pipeline against one vessel leg counted by hand. The dominant signals agreed — zero zooplankton and a load dominated by carbon and fine unresolved material — while the split between plastic and phytoplankton diverged, and we therefore treat that partition as provisional. Because visual identification of these small, degraded particles by non-specialists is necessarily subjective, we do not rely on the crew hand-logs quantitatively; the objective confirmation of the zooplankton result comes instead from the surface net tow (Sect. 2.8, Table 2). “Black carbon” here is an optical description — dark, colourless particles — and could include sediment, shadow or dark plastic; confirming its composition requires spectroscopy. These are microscope images from an opportunistic citizen-science programme, but the sampling hardware was standardised and a single microscope design was used across all vessels, so between-instrument optical variability is limited and the main residual variability is in operator technique and illumination. Airborne contamination is constrained by the cartridge design: the filter stays capped from collection until analysis and is exposed only for the few minutes when the plate is removed and placed under the microscope, and procedural blanks run by the lead author showed no obvious contamination. The volunteer crews, however, were not instructed to run their own blanks, so airborne contamination of the citizen-collected samples cannot be fully excluded — the microfibre counts in particular should be read with that caveat.

https://doi.org/10.5194/egusphere-2026-3979
Preprint. Discussion started: 29 July 2026

2.8 Independent confirmation by surface net tow, day and night

To test whether the near-absence of zooplankton in the surface grab samples was an artefact of the small sampled volume, a concentrating plankton net was towed at the surface in the mid-Atlantic. A 120 µm mesh net of 0.30 m mouth diameter was towed at the surface at 1 to 2 knots for 10 minutes per haul; each haul therefore strained roughly 43,600 litres (mouth area 0.071 m² × ~617 m towed). Because many zooplankton migrate downward by day and rise toward the surface at night, the net was towed in two sets: ten hauls in daylight (12:00–15:00, local time) and four after dark. This removes the main alternative explanation for the image survey: the surface scarcity is not simply an effect of small sample volume. Two methodological caveats remain — the 120 µm mesh retains larger taxa while passing the smallest copepods and nauplii, and filtered volume is computed from tow geometry rather than a flow-meter. A surface zooplankton stock of 0.2–0.5 per cubic metre, day and night (night density ~2× daytime, consistent with diel vertical migration), nonetheless sits far below densities typical of productive open ocean.

2.9 Comparison with previous surveys of the region

Systematic plankton and particle surveys of the open equatorial and trade-wind Atlantic are sparse, and — crucially — those that exist have run **meridionally**: north–south, along a line of longitude, crossing the equator and cutting across latitudinal climate zones. Like the GOES crossing, these meridional lines sampled open-ocean water well off the continental shelf — the Atlantic Meridional Transect and the 20°W line run directly through the oligotrophic subtropical gyres — so the contrast drawn here is between comparably unproductive open waters, not between a productive shelf and the open ocean. The GOES survey, by contrast, ran **zonally**: east–west, parallel to a line of latitude, following the trade-wind crossing from North Africa to the Caribbean at roughly constant latitude. The principal sustained effort in the region, the Atlantic Meridional Transect, runs north–south between the United Kingdom and the South Atlantic (Aiken et al., 2000); Woodd-Walker et al. (2000) characterised surface zooplankton along a 20°W meridional transect; and Vereshchaka et al. (2017) synthesised zooplankton along the Atlantic meridional axis. For plastics, Pabortsava and Lampitt (2020) sampled beneath the Atlantic surface along the meridional AMT line, and Cózar et al. (2014) drew on a global circumnavigation rather than any single east–west section. Because every one of these prior surveys runs along a longitude, or is a global compilation, the GOES survey is, to our knowledge, the first — and to date the only — survey to measure plankton and microplastic together along a zonal (east–west) transect parallel to the equator, from North Africa to the Caribbean.

2.10 Comparison with other methods

If the citizen-science imaging method is to stand as a result in its own right, it must be set against conventional tools — plankton nets, pumps, the Continuous Plankton Recorder and laboratory microscopy or flow-cytometry — which sample with standardised gear and calibrated volumes but at higher cost and usually integrated over depth. The GOES method inverts that balance: it resolves the

https://doi.org/10.5194/egusphere-2026-3979
Preprint. Discussion started: 29 July 2026

20–200 µm fraction exactly at the air–sea interface, delivers dense spatial coverage across an under-sampled basin at very low cost, and scales to a distributed volunteer fleet. Its weaknesses, stated frankly, are that the volunteer crews were not asked to run their own procedural blanks — although blanks run by the lead author showed no obvious contamination, and a single common microscope design was used across all vessels — leaving possible airborne fibre contamination, an optical "black carbon" class awaiting spectroscopic confirmation, and a provisional plastic-versus-phytoplankton partition, each mapped to a specific refinement written into the next campaign (Sect. 8).

2.11 Survey at a glance

Class	Stations present	Conc. /L (median; 95th pct)	Notes
Zooplankton	6.2%	0; 2	44 objects total; median 328 µm
Phytoplankton	81.8%	10; 70	pigmented aggregates, diatoms
Black (combustion) carbon	89.8%	12; 99	3,559 particles; median 31 µm
Microplastic particles	69.9%	5; 50	coloured fragments
Microfibres	22.4%	0; 6	median fibre length 204 µm

Table 1. Survey at a glance. Per-station concentrations (a full 0.5-litre sample is counted across all five Ø5 mm apertures at every station, so per litre ≈ the whole-station count × 2) are summarised across all 352 stations as the median and 95th percentile; the distributions are strongly right-skewed, and the busiest stations reach several hundred per litre for phytoplankton, black carbon and microplastic. Counts include only particles ≥20 µm. The particle-class totals quoted (e.g. 3,559 black-carbon particles) are from the full 51,547-particle inventory.

Set	Hauls	Zooplankton (m^{-3})
Daytime (12:00–15:00)	10	~0.2
Night (after dark)	4	~0.4 (≈2× daytime)

Table 2. Surface net-tow confirmation of zooplankton scarcity, day and night (120 µm mesh, 0.30 m mouth, ~2 kn, 10 min per haul). Densities assume complete filtration and are upper bounds; night density ~2× daytime, consistent with diel migration, yet remains below 0.5 m^{-3}.

Vessel	Stations	Longitude span	Latitude	Sampling dates	% zoo	% carbon
Copepod	110	-17°W to 56°W	12–24°N	Jan–Feb 2022	0.0	82.7
Emma	78	-9°W to 62°W	2–50°N	Jan–Feb 2022; May 2023	2.6	96.2
Misty Blue	35	-15°W to 61°W	12–28°N	Jan–Feb 2022	8.6	91.4
Eleuthera	33	-15°W to 67°W	12–28°N	Jan–Feb 2022	12.1	93.9
Yolo	27	-18°W to 59°W	13–24°N	Jan–Feb 2022	29.6	70.4
Ya	33	-26°W to 52°W	4–17°N	Jan–Feb 2022	6.1	97.0
DanceMe	33	-25°W to 60°W	6–17°N	Jan–Feb 2022	9.1	100.0
Jiyu	3	-16°W to 17°W	28–28°N	Jan–Feb 2022	0.0	100.0

Table 3. Participating vessels, their station counts, longitudinal and latitudinal spans, sampling dates, and the percentage of stations at which zooplankton and black carbon were detected. All vessels sampled the trade-wind crossing

10

https://doi.org/10.5194/egusphere-2026-3979
Preprint. Discussion started: 29 July 2026

contemporaneously in January–February 2022 (timing referenced to the GPS-tagged Copepod crossing, Fig. 1); Emma additionally sampled a higher-latitude North Atlantic return leg (to 50°N) in May 2023.

3. Sources of marine pollution and their implications

The SML attracts lipophilic "forever" chemicals, microplastics and hydrophobic black-carbon soot from the incomplete combustion of fossil fuels and biomass. Measured concentrations of toxic chemicals in the SML can be many times higher than in the water below (Wurl and Obbard, 2004), and a meta-analysis of surface-microlayer sampling finds organic matter systematically enriched there, with median enrichment factors of about three for particulate organic carbon and above two for nitrogen-rich compounds (Silva et al., 2026), so the layer acts as an accumulator at the precise interface where plankton live. Hydrophobic black carbon and plastic particles preferentially adsorb these lipophilic chemicals and can carry them into the base of the food web (Bond et al., 2013; Ziccardi et al., 2016). Weathered plastic recovered from the open sea can concentrate persistent organic pollutants such as PCBs and DDE to levels up to about a million times those of the surrounding seawater, and that adsorbed burden rises the longer the particle has drifted at sea (Mato et al., 2001). Partially combusted carbon behaves much like plastic in this respect, a point that has been largely overlooked. Both classes are present across the open Atlantic far from land (Cózar et al., 2014; Pabortsava and Lampitt, 2020), so this is an open-ocean phenomenon, not only a coastal one. This same burden of combustion and chemical pollution is, beyond the ocean, a leading environmental cause of human disease and premature death, so that cutting it serves planetary and human health together (Landrigan et al., 2020; Fuller et al., 2022). Beyond the microscopic fraction sampled here, macroplastic ingestion is itself now a quantified cause of mortality in seabirds, marine mammals and sea turtles, and at surprisingly small ingested doses (Murphy et al., 2025).

The sea surface does not merely store this pollution; it exports it. Rising bubbles scavenge the microlayer and burst at the surface, ejecting film-bound material into the air as sea-spray aerosol (O'Dowd et al., 1997; O'Dowd et al., 2004); because the SML concentrates microplastic, nanoplastic and their adsorbed lipophilic chemicals far above the water beneath (Wurl and Obbard, 2004; Ziccardi et al., 2016), that spray is correspondingly enriched. Microplastic is now measured in the remote marine atmosphere (Trainic et al., 2020) and quantified as an ocean-sourced limb of a global atmospheric plastic cycle (Brahney et al., 2021); aloft it can seed cloud and ice (Aeschlimann et al., 2022) before returning to land and sea in rain and snow, from remote mountain catchments to polar snow (Allen et al., 2019; Bergmann et al., 2019; Aves et al., 2022). The old water-industry adage that "the solution to pollution is dilution" does not hold for this lipophilic, film-bound class of contaminant: instead of dispersing into the ocean's volume, the material partitions into the surface skin and is redistributed rather than diluted away. And because these lipophilic "forever" chemicals do not break down, their environmental concentration does not fall but climbs year on year for as long as they keep entering the ocean — the reverse of the dilution the adage assumes.

11

https://doi.org/10.5194/egusphere-2026-3979
Preprint. Discussion started: 29 July 2026

4. The surface microlayer, aerosols, clouds and evaporation

The SML is built from phytoplankton lipids and surfactants (Garrett, 1967; O'Dowd et al., 2004). It feeds the marine aerosols that clouds condense upon (O'Dowd et al., 1997), and at the same time it slows the escape of water from the sea surface and the loss of heat to the air (Garrett, 1967; Cunliffe et al., 2013; Engel et al., 2017). That the microlayer measurably brakes air–sea exchange is now established in the ocean itself: natural sea-surface surfactants reduce the in-situ air–sea gas-transfer velocity by about 23% across wide areas of the ocean, with a further ~62% reduction inside slicks, lowering the global air–sea CO_2 flux by roughly a fifth (Mustaffa et al., 2020); in the Atlantic specifically, biological surfactants have been shown to suppress air–sea CO_2 exchange directly (Pereira et al., 2018), and recent work linking surfactant surface coverage to gas exchange confirms that natural microlayer films can reduce the CO_2 transfer velocity by up to roughly half (Asmussen-Schäfer et al., 2026). Evaporation and the loss of latent heat cross the same interfacial film, so a sea surface stripped of its biological skin should shed moisture and heat more freely. Losing that film is the removal of a biological brake on air–sea exchange, not a minor detail of surface chemistry. A healthy film cools the surface, encourages cloud and rain, and keeps humidity in check. Strip it away and evaporation and water vapour can rise while cloud cover falls. And when cloud does form under these conditions, the higher humidity — combined with the atmospheric dust and pollution particles that act as cloud-seeding nuclei — can favour larger, more energetic storm clouds, stronger winds and torrential downpours in place of the gentler, more frequent rain a healthy surface would encourage. A shift toward fewer but more violent events is the emerging signature of a warming, moisture-laden atmosphere: attribution studies tie anthropogenic warming and enhanced cross-equatorial moisture transport to the record-shattering 2022 Pakistan monsoon floods (You et al., 2024), and to the historic 2022 Mediterranean derecho, whose squalls gusted to about 220 km h^{-1} over Corsica and which a preindustrial atmosphere would not have generated (González-Alemán et al., 2023). We cite these as illustrations of the direction of change in a moister atmosphere, not as events attributable to the surface-microlayer mechanism proposed here. Since the ocean supplies most of that atmospheric moisture — about 86% of global evaporation, and the ultimate source of the majority of precipitation even over land, with terrestrial evapotranspiration and biogenic aerosol from vegetation accounting for most of the remainder (Gimeno et al., 2012) — the physical and biological condition of the sea surface is a climate variable in its own right, and one that carbon-only models leave out.

Independent reanalysis is at least consistent with this picture. Area-weighted ERA5 fields for the North Atlantic show that the seasonal amplitude of total-column water vapour — the size of its month-to-month swing — has increased in every latitude zone since 1940, most strongly at mid-latitudes, while the amplitude of cloud cover has not changed (Fig. 6). Temperature ultimately governs how much moisture the air can hold, through the Clausius–Clapeyron relation, and it sets both the long-term rise in humidity and the breadth of its seasonal cycle. But temperature acts slowly. We propose that the microlayer acts on a much shorter timescale — hours to days — regulating the rate at which the surface

https://doi.org/10.5194/egusphere-2026-3979
Preprint. Discussion started: 29 July 2026

gives up its water, and with it the short-term rate of change and the amplitude of near-surface humidity: a sea surface stripped of its biological film would shed moisture faster and let humidity swing more sharply, which is the behaviour the widening amplitude hints at. That the rise is strongest at mid-latitudes may itself fit this reading: these are historically the more productive waters, where a richer plankton community once maintained a more developed microlayer, so its degradation would represent the largest loss of that biological brake — and hence the sharpest increase in humidity amplitude. Monthly reanalysis cannot resolve a sub-monthly, film-scale process, so this remains a hypothesis rather than a result.

A companion signal that would be expected is, however, missing. If humidity, temperature and the amplitude of their oscillations are all rising together, cloud cover might be expected to rise with them; instead it is flat or slightly declining. A partial explanation is that cloud formation in this basin is limited not by the supply of water vapour but by the availability of cloud condensation nuclei, which here is dominated by aerosol pollution and wind-blown Saharan dust rather than by the biogenic aerosol that healthy plankton once supplied (O'Dowd et al., 1997; O'Dowd et al., 2004). A large part of that biogenic supply is sulfurous: dimethyl sulfide (DMS) released by phytoplankton — coccolithophores prominent among them — oxidises in air to sulfate particles that seed cloud droplets, the negative feedback at the heart of the long-debated CLAW hypothesis (Charlson et al., 1987). Whether that feedback is strong enough to regulate global climate is contested (Quinn and Bates, 2011), but its direction is not: a surface ocean losing its coccolithophores and its living microlayer supplies fewer biogenic nuclei, so more moisture can accumulate as vapour without being converted into cloud. A surface that is growing warmer and wetter, with ever sharper humidity swings, yet no cloudier, is at least consistent with a weakening of the biological control over both evaporation and cloud seeding — though the present data cannot prove it.

13

https://doi.org/10.5194/egusphere-2026-3979
Preprint. Discussion started: 29 July 2026

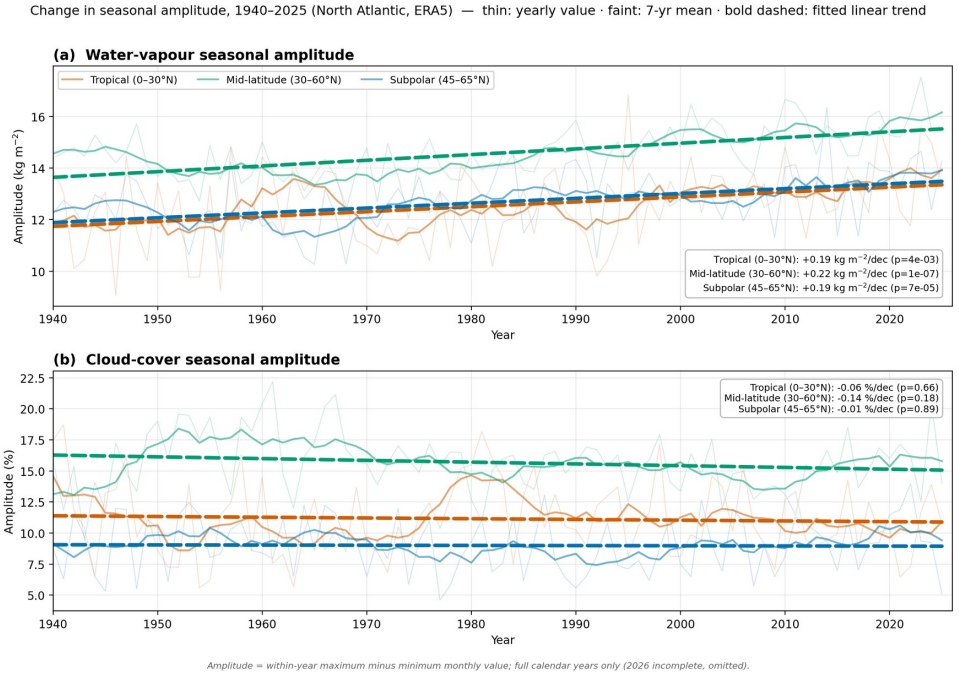

Figure 6. Change in the seasonal amplitude of (a) total-column water vapour and (b) cloud cover over the North Atlantic by latitude zone, 1940–2025, from ERA5 monthly reanalysis (area-weighted zonal means; thin line, yearly amplitude; bold dashed, fitted linear trend). Amplitude is the within-year maximum minus minimum. Water-vapour amplitude rises significantly in every zone (+0.19 to +0.22 kg m^{-2} per decade); cloud-cover amplitude shows no significant trend. Shown as physical context for the surface-microlayer hypothesis; the reanalysis cannot itself resolve the microlayer.

Two water-quality parameters that oceanography rarely records may also shape how the material documented here behaves: the redox potential of the water and the zeta potential — the surface charge — of the particles suspended in it. Surface charge governs whether suspended particles, plankton and microplastic alike, repel one another and stay dispersed, clouding the water, or lose that repulsion, aggregate and sink (Parrella et al., 2024); and, consistent with an increasingly turbid surface, the global ocean has measurably darkened over the two decades to 2022, shrinking the sunlit photic zone (Davies and Smyth, 2025). We raise, as a hypothesis for future work rather than a result of this survey, the possibility that a deoxygenating, more reducing surface shifts this balance towards stable turbid suspensions, and that the same biological collapse which consumes oxygen also releases CO_2 and depresses pH, so that deoxygenation and acidification advance together (Cai et al., 2011; Breitburg et al., 2018). Neither redox nor zeta potential was measured here; both would be worth adding to future surface-microlayer work.

14

https://doi.org/10.5194/egusphere-2026-3979
Preprint. Discussion started: 29 July 2026

5. Ecosystem regime shift and ocean acidification

Toxic loading affects grazing zooplankton (Desforges et al., 2015; Ma et al., 2020); the survey's near-total absence of animals is consistent with heavy grazer loss, after which phytoplankton may bloom and sink un-grazed. Because zooplankton are also a principal route by which iron is regenerated in the surface layer — grazing, sloppy feeding and excretion return bioavailable iron to the euphotic zone (Barbeau et al., 1996) — their loss can carry a patch from that transient bloom toward iron limitation, as the iron bound in the sinking, ungrazed cells is exported rather than recycled. This is a locally generated route into the high-nutrient, low-chlorophyll (HNLC) condition seen across large parts of the open ocean, where macronutrients remain abundant but phytoplankton growth is limited chiefly by iron (Tyrrell et al., 2005). As primary production changes, less carbon may be fixed at the surface and dissolved CO_2 rises; microplastic loading may itself further weaken the biological carbon pump (Shen et al., 2020). The coccolithophores and diatoms that build the SML are also among the plankton least able to tolerate falling pH (Riebesell et al., 2000; Hönisch et al., 2012); lose them and the film thins further, tightening a loop between acidification, plankton loss and evaporation. On present trends, surface pH could fall below about 7.95 within a few decades (Hönisch et al., 2012). Whether these strands could tighten into a basin- or ocean-scale regime shift, and how quickly, is genuinely uncertain, and the present data do not settle it.

This low-chlorophyll condition is not merely inferred from the sampling: independent satellite ocean colour confirms it. Across the trade-wind transect the mean surface chlorophyll-a concentration is only about 0.09 mg m^{-3}, and the great majority of the crossing lies below the 0.15 mg m^{-3} level conventionally taken to mark oligotrophic water, so the near-absence of surface animals recorded here occurs within some of the least productive open water in the North Atlantic (Fig. 7). Elevated chlorophyll is confined to the Mauritanian and equatorial upwellings and the continental margins, well away from the sampled crossing, and the decade mean (2006–2015) gives an almost identical transect value, so the pattern is climatologically stable rather than a single-year anomaly. An entirely independent instrument therefore agrees with the microscopy that this is biologically impoverished water. Satellite colour cannot, of course, distinguish naturally oligotrophic gyre water from water depleted by the mechanisms proposed here; it establishes the low-productivity setting, not its cause.

15

https://doi.org/10.5194/egusphere-2026-3979
Preprint. Discussion started: 29 July 2026

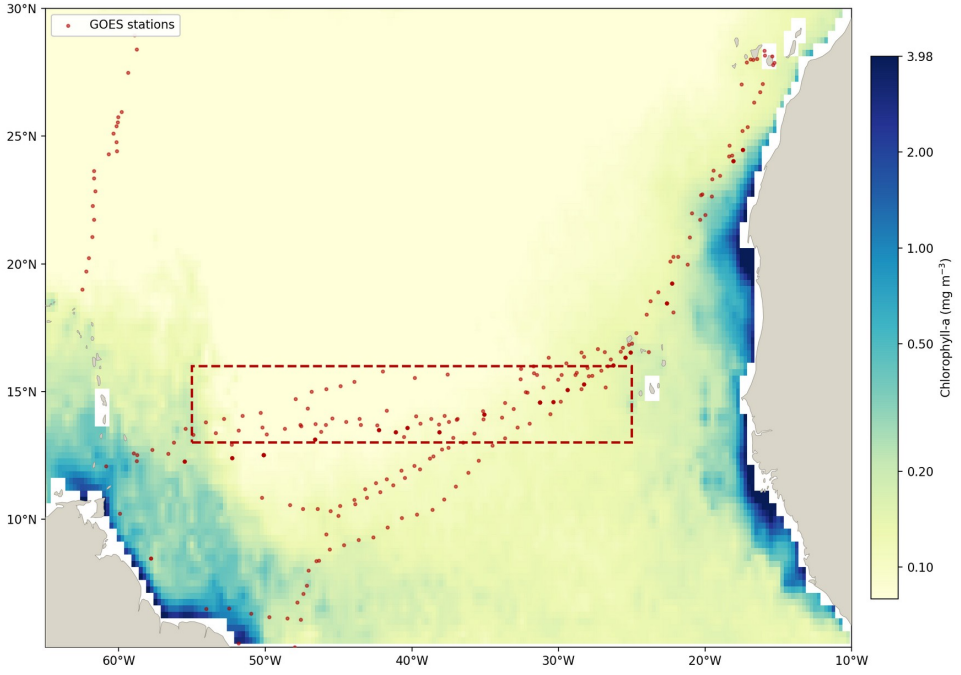

Figure 7. Satellite chlorophyll-a concentration (MODIS-Aqua, 2010; logarithmic colour scale) across the study region, with the GOES sampling stations (red) and the trade-wind transect box (dashed). The crossing runs through the oligotrophic core of the subtropical gyre — transect median ≈ 0.09 mg m^{-3}, the great majority below the 0.15 mg m^{-3} oligotrophic threshold — while elevated chlorophyll is restricted to the Mauritanian and equatorial upwellings and the continental margins. A decade mean (2006–2015) yields an almost identical transect median, confirming the pattern is climatologically stable. Chlorophyll-a data © NASA Earth Observations (MODIS-Aqua). Coastlines © Natural Earth.

5.1 Sargassum

There should be in the region of 1 to 2 million tonnes of Sargassum crossing the equatorial Atlantic from Africa to the Caribbean. However, due to eutrophication from the Amazon, Gambia and Congo rivers, together with nutrient-rich run-off, the biomass of the Great Atlantic Sargassum Belt is now of the order of tens of millions of tonnes (Wang et al., 2019; Lapointe et al., 2021). Yachts in the project were frequently caught in giant mats of this pelagic macrophyte, which competes with phytoplankton for phosphate and other nutrients (Lapointe et al., 2021). As phosphate falls, Sargassum increasingly takes up arsenate in place of phosphate — the two are taken up through the same phosphate transporter — so that by the time it reaches the Caribbean the tissue is heavily loaded with arsenic (Devault et al., 2020; Rodríguez-Martínez et al., 2020; McGillicuddy et al., 2023). Because a plant switches to arsenate only once phosphate has become scarce, that arsenic burden is itself indirect evidence — although we did not measure dissolved phosphate or arsenate — that phosphate is drawn down to very low levels across the equatorial belt where the Sargassum grows. A macrophyte bloom of this mass, monopolising phosphate and other nutrients at the surface, would leave little for the phytoplankton that draw on the same pool,

16

https://doi.org/10.5194/egusphere-2026-3979
Preprint. Discussion started: 29 July 2026

and with them the zooplankton that graze them. Nutrient stripping by the Sargassum belt is therefore a further, independent candidate explanation for the near-absence of plankton reported here, alongside the pollutant and microlayer mechanisms, and one that a targeted phosphate and arsenate survey could test directly. This mechanism also carries a temporal dimension that bears directly on the comparison with earlier surveys. The Great Atlantic Sargassum Belt is a recent phenomenon, essentially absent before about 2011 and expanding to tens of millions of tonnes only in the years since (Wang et al., 2019); the meridional transects against which our low counts are set (Aiken et al., 2000; Woodd-Walker et al., 2000) were made before the belt emerged. The rise of a basin-scale macrophyte bloom that monopolises surface nutrients could therefore contribute to the gap between the higher plankton abundances those surveys recorded and the near-absence found here, so that part of the contrast may reflect a genuine change in the equatorial Atlantic over the intervening two decades rather than sampling differences alone.

5.2 Microplastics, primary producers and ocean oxygen

Because the surface layer we sampled is where the ocean's most abundant photosynthetic organisms live, the pollutant load documented here bears directly on marine oxygen production. Laboratory exposure shows that leachates from common plastics impair the growth and oxygen production of Prochlorococcus, the single most abundant marine photosynthetic bacterium (Tetu et al., 2019). To convey the scale of what is at stake, Prochlorococcus numbers of order 10^{27} cells across the world ocean — more, by a factor of billions, than the roughly 4×10^{17} seconds that have elapsed since the Big Bang — yet at about 0.6 µm per cell it escaped detection until the mid-1980s, passing through the >100 µm nets of conventional plankton surveys until it was identified by Chisholm et al. (1988); it is thought to generate of order a quarter of marine primary production and, with it, a comparable share of the ocean's oxygen supply and biological carbon fixation, so that its sensitivity to plastic leachates carries a correspondingly large potential cost. At a global scale, a recent meta-analysis estimates that microplastic pollution measurably depresses photosynthesis across aquatic and terrestrial primary producers, implying substantial losses of marine primary production and oxygen output (Zhu et al., 2025). Microplastics can also lower oxygen indirectly: model experiments indicate that zooplankton grazing on microplastic re-routes export production in a way that accelerates the ongoing global loss of ocean oxygen (Kvale et al., 2021). Plastic is an emerging, additional stressor that compounds the dominant, well-quantified drivers of ocean deoxygenation, warming and eutrophication.

5.3 Multiple stressors and the risk of a regime shift

The biological significance of regional surface-pH minima depends on how long low-pH conditions persist, and sustained exposure reduces the fecundity and survival of plankton and other calcifying organisms, amplified where acidification coincides with warming (Kroeker et al., 2013). Regional acidification is already measurable across the basin and its margins: corrosive, CO_2-enriched water upwells onto continental shelves (Feely et al., 2008), and sustained acidification has been documented

17

https://doi.org/10.5194/egusphere-2026-3979
Preprint. Discussion started: 29 July 2026

for the Greater Caribbean (Gledhill et al., 2008) and, as a semi-enclosed comparison, the Mediterranean (Hassoun et al., 2015), while natural CO_2 seeps provide in-situ analogues of how falling pH restructures plankton communities (Dando et al., 1995). For the trade-wind corridor itself, open-ocean surface pH remains in the low 8.0s: the ESTOC time series off the Canary Islands averages about 8.08 and the PIRATA array in the western tropical Atlantic about 8.06, both falling by roughly 0.02 pH units per decade (González-Dávila and Santana-Casiano, 2023; Assis et al., 2024). Its eastern, upwelling-influenced margin already reaches far lower, however: seasonal upwelling of carbon-rich water off Northwest Africa near Cape Blanc draws surface pH down to about 7.8, with aragonite saturation near 1.5 (Jamal et al., 2025) — the corrosive endpoint the open ocean is projected to approach only decades hence, present today at the productive edge the crossing passes through. These are bulk-water values; the sea-surface microlayer's own inorganic-carbon chemistry can differ from the water beneath and swings strongly over the day — enough that neglecting the night biases air–sea CO_2 flux estimates by a third to a half — so the pH experienced at the very skin where the plankton live is modulated at the microlayer itself (López-Puertas et al., 2025). This stress acts together with the toxic-chemical and particulate load documented earlier; multiple stressors interact and can compound one another (Kroeker et al., 2013; Tetu et al., 2019). Sustained acidification and warming also restructure the plankton community, reducing the proportion of diatoms and favouring dinoflagellates (Dutkiewicz et al., 2015). Consistent with large-scale change, more than half of the global ocean — approximately 56% — has become measurably greener over two decades (Cael et al., 2023), and an integrated assessment of Northeast-Atlantic plankton reported general declines in phytoplankton biomass and zooplankton abundance, with no pelagic habitat achieving "Good" status (McQuatters-Gollop et al., 2026). GOES interprets these converging trends as an early warning of a possible large-scale regime shift (Beaugrand et al., 2019); whether it could unfold within a decade is uncertain and not established by the present evidence.

6. Carbon dioxide and marine biodiversity

Carbon dioxide still matters. Even at net zero, the CO_2 already in the air would keep acidifying the ocean (Hönisch et al., 2012; Jiang et al., 2019). The case here is additive, not dismissive: cutting carbon is necessary but not sufficient. Leave in place the pollution harming surface plankton, and the SML may keep degrading. Enhanced weathering — spreading finely ground silicate minerals such as olivine, whether on land or in coastal seas, to draw down CO_2 and raise alkalinity — has been proposed, but its scale, cost and ecological side-effects remain highly uncertain, and we raise it only as something to be evaluated.

7. Recommendations

Continue and accelerate carbon mitigation, but treat pollution elimination as a parallel climate measure of equal urgency. Eliminate discharge of lipophilic "forever" chemicals, plastic and black-carbon soot; treat all wastewater; and transition towards regeneration of ecosystems and biodiversity on land and at

18

https://doi.org/10.5194/egusphere-2026-3979
Preprint. Discussion started: 29 July 2026

sea. The scale of the wastewater gap is stark: roughly 80% of the world's wastewater is returned to the environment with no treatment at all (WWAP, 2017), and even in the high-income countries that do treat it, only a small proportion of plants — of order a tenth — employ the tertiary or advanced stages capable of removing microplastic and lipophilic chemicals. Evaluate raising seawater alkalinity, subject to full assessment of efficacy and side-effects. Establish standardised, calibrated surface-microlayer monitoring — building on the citizen-science method here but adding laboratory particle confirmation (FTIR/Raman), procedural blanks and replication.

7.1 Scaling up: satellite radar of the sea surface

The point observations here could be extended to the whole ocean surface by remote sensing. The biogenic microlayer and its surfactant films damp short capillary waves and smooth the sea surface; in-situ measurements confirm the biopolymer-rich film sharply reduces surface roughness at low wind, collapsing above roughly 6 m s^{-1} (Engel et al., 2026). Synthetic-aperture radar (SAR) measures exactly this roughness, and has already been used to map ocean "microplastic" from surface-roughness anomalies (Evans and Ruf, 2022). We suggest, however, that the radar is not sensing plastic directly: at realistic concentrations microplastic does not measurably damp capillary waves, whereas phytoplankton lipids and exopolymers do, so a SAR slick is in effect a bloom detector. That such slicks coincide with high microplastic is exactly what our mechanism predicts — where pollution removes the grazing zooplankton, the ungrazed phytoplankton bloom and the surfactants they release smooth the surface (Desforges et al., 2015; Tetu et al., 2019; Ma et al., 2020). Because zooplankton also recycle iron to the surface through grazing and excretion (Barbeau et al., 1996), their loss lets the iron in the sinking, ungrazed bloom be exported rather than replenished, driving the patch toward iron-limited, high-nutrient, low-chlorophyll conditions (Tyrrell et al., 2005). HNLC water is no marginal case — roughly a quarter of the global ocean, and most of the Southern Ocean (Basterretxea et al., 2023) — so a process that manufactures fresh iron-starved patches wherever pollution strips the grazers could extend such conditions well beyond the classical iron-limited regions. The low-chlorophyll ocean is in any case already growing: the least-productive oligotrophic waters — including the subtropical gyre this transect crossed — expanded at 0.8 to 4.3% per year across the Pacific and North Atlantic over the satellite era, faster than stratification models had predicted (Polovina et al., 2008). A SAR-bright, surfactant-smoothed, plastic-associated patch is then not a map of plastic but a snapshot of a plankton community tipping — grazers gone, a transient bloom, iron recycling failing beneath it — and a testable one, predicting a sequence of grazer loss, a chlorophyll pulse, then declining surface iron. We therefore recommend evaluating satellite radar of sea-surface roughness as a complement to the in-situ imaging here, with the citizen-science stations as ground-truth calibration, to detect at basin scale where the plankton community is beginning to tip (Beaugrand et al., 2019).

This bears directly on ocean iron fertilization. Proposed as a way to raise phytoplankton and, through them, zooplankton productivity by relieving iron limitation in HNLC waters, the fertilization trials of

https://doi.org/10.5194/egusphere-2026-3979
Preprint. Discussion started: 29 July 2026

the past twenty-five years have largely failed: added iron raised primary production but, outside a single Southern Ocean experiment, delivered no durable carbon export (Yoon et al., 2018). The reason may not be the iron. If these waters are constrained less by iron than by their changing carbonate chemistry and the burden of microplastic and partially combusted carbon — with its adsorbed lipophilic toxicants — of the kind documented here, then adding iron cannot restore a functioning community, and the bloom it provokes is as likely to be transient or toxic as productive (Trick et al., 2010). The near-absence of surface plankton reported here is thus a direct caution for such schemes: where water chemistry and pollutant load are the true constraints, it is removing that burden, not adding iron, that is the precondition for recovery.

8. Conclusion

Across 352 stations and 51,547 classified particles, the trade-wind Atlantic surface held almost no animal plankton above 20 µm, a great deal of combustion and plastic residue, and a particle field dominated by its smallest sizes. Not every step in the surface-microlayer hypothesis is settled, and throughout we have tried to mark clearly where the evidence ends and interpretation begins. But a surface ocean this empty of plankton and this laden with anthropogenic particles is, on any reading, a stressed system — and stressed systems of this kind are the ones that tip (Beaugrand et al., 2019; IPBES, 2019).

Emissions must fall, and urgently. Yet carbon mitigation alone will neither halt ocean acidification nor rebuild the microlayer: the discharge of black carbon, lipophilic “forever” chemicals and plastic has to fall alongside it. The argument is additive rather than contrarian — cutting carbon is necessary but not sufficient. The reason it matters beyond the trade-wind belt is that marine plankton are the ocean’s, and in large part the planet’s, life-support system: they generate an estimated 50 to 80% of the oxygen in every breath, with the ocean supplying roughly half of global net primary production (Field et al., 1998), anchor the marine food web, and drive the biological carbon pump. Remarkably, this planetary life-support rests on a very small standing stock: the ocean’s primary producers amount to only about 1 Gt of carbon — against roughly 450 Gt in land plants — yet sustain a still larger mass of consumers above them, an inverted biomass pyramid held up only by the phytoplankton’s rapid turnover (Bar-On et al., 2018). A climate framed around carbon dioxide alone leaves this biology out, and with it a second, biologically governed control on the sea surface.

The stakes, then, are not only climatic. A disrupted climate is survivable; the unravelling of the fragile living systems that produce our oxygen and feed the ocean is a hazard of a different kind. But plankton rebound quickly once the pressure is lifted (Laws, 2013; Bar-On et al., 2018), so this is a loss that can still be arrested. On the evidence presented here, reducing pollution is not an afterthought to decarbonisation but a climate measure of comparable standing. Carbon tunnel vision — the reflex to treat CO_2 as the only lever — has kept that second control out of sight; restoring marine life belongs alongside cutting carbon, not behind it.

20

https://doi.org/10.5194/egusphere-2026-3979
Preprint. Discussion started: 29 July 2026

Appendix A: Methods

Sampling filter

The sampling filter is shown in Fig. A1. It is a self-contained cartridge — a Ø50 × 380 mm PVC tube with a slip-over end cap, housing two acrylic filter plates (each with one central and four Ø5 mm holes on a Ø20 mm pitch circle) within a standard PVC solvent-weld pipe union, and suspended on a Kevlar cord (filter designed by Dr Jesús Ramón Barriuso Díez of Calplas, in the Basque Country of Spain; full build details are given in the GOES field guide for volunteers, https://goesfoundation.com/water-sampling-field-guide-for-volunteers/). The design draws a precise 0.5-litre sample of seawater on each fill, independent of the vessel's speed through the water, and because it hangs from its cord it filters vertically. It therefore provides an accurate, quantitative measure of the particle content of a known 0.5-litre volume of water, capturing everything larger than 20 µm.

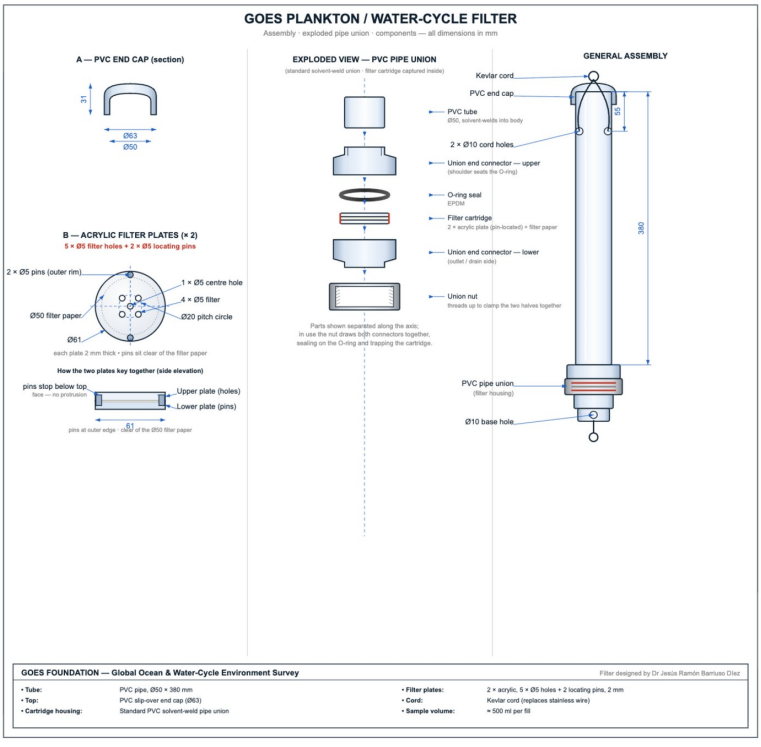

Figure A1. The GOES plankton / water-cycle filter: general assembly, exploded view of the standard PVC pipe-union housing, and the two acrylic filter plates (one central + four Ø5 mm filter holes on a Ø20 mm pitch circle, keyed by two Ø5 mm locating pins on the outer rim, clear of the Ø50 mm filter paper). The cartridge draws a fixed 0.5-litre sample independent of the vessel's speed through the water and, suspended on its Kevlar cord, filters vertically, capturing all particles above 20 µm. Designed by Dr Jesús Ramón Barriuso Díez (Calplas, Basque Country, Spain).

Surface samples were collected by participating crews at ~12-hour intervals (12:00 and 24:00 hrs, local time), filtered to ~20 µm, and photographed on digital microscopes at a 5 mm field of view, with

21

https://doi.org/10.5194/egusphere-2026-3979
Preprint. Discussion started: 29 July 2026

position, date and time logged. Positions were taken from image GPS (for the geotagged subset) or from the field spreadsheet. Per-image timestamps are available only for the Copepod crossing (8 January – 3 February 2022); the sampling dates of the other vessels, which crossed contemporaneously, are referenced to that crossing (Fig. 1). Images were analysed in OpenCV: Hough-circle aperture detection, then segmentation by combined background-subtraction and saturation thresholds; connected components ≥20 µm (scaled by 5 mm / image width) were classified by elongation, saturation, hue and darkness, with unresolved objects left unidentified, and every particle sized. The pipeline was cross-checked against one hand-counted leg. Net-tow validation: a 120 µm plankton net (0.30 m mouth) was towed at the surface at ~2 knots for 10 min per haul — ten daytime and four night hauls, mid-Atlantic; filtered volume was computed as net mouth area × tow distance. Per-station counts, all particle sizes and the crew logs accompany this paper as a supplementary workbook (GOES_ALL_DATA.xlsx).

Data availability

The complete data set underlying this study — the per-station particle counts, the individual particle-size measurements and the crew field logs — is provided in the supplementary workbook (GOES_ALL_DATA.xlsx) and is openly archived in the Zenodo repository (https://doi.org/10.5281/zenodo.21477682; Dryden et al., 2026). The crew hand-logs are included for transparency; because visual identification of small, degraded particles by non-specialists is subjective, these hand counts are provided as qualitative context only and are not used in the quantitative analysis, which rests on the automated image pipeline and the surface net tow. The ERA5 reanalysis fields used for the water-vapour and cloud figures are freely available from the Copernicus Climate Change Service (C3S) Climate Data Store, and the MODIS-Aqua chlorophyll-a product from NASA Ocean Color.

Code availability

The data-processing and figure-generation code used to produce the figures, tables and reference list of this study is openly archived at Zenodo (https://doi.org/10.5281/zenodo.21477682). The particle-classification image pipeline (OpenCV: filter-aperture detection, segmentation, sizing and classification of the microscope images) is available from the corresponding author on reasonable request.

Author contributions

H.D. conceived and led the GOES project, designed the sampling protocol, and led the analysis and writing. D.D. contributed to the study design and to the manuscript. The authors skippered the sailing vessel Copepod, which provided the GPS-tagged reference crossing. The participating vessel crews collected the remaining field samples and microscope images. All authors reviewed and approved the final manuscript.

https://doi.org/10.5194/egusphere-2026-3979
Preprint. Discussion started: 29 July 2026

Competing interests

The authors are associated with the GOES Foundation, a not-for-profit organisation originally based on the sailing vessel Copepod and now located at www.seahorsepoint.org in Bocas del Toro, Panama. They declare no financial competing interests.

AI-assistance statement

The data analysis and figure generation of this manuscript were carried out with the assistance of a generative-AI system (Anthropic's Claude). All data, interpretations and conclusions are the authors' own; the authors verified the analyses and references and take full responsibility for the content.

Acknowledgements

We thank the volunteer skippers and crews of the eight participating vessels — Copepod, Emma, Misty Blue, Eleuthera, Yolo, Ya, DanceMe and Jiyu — without whom this survey would not have been possible; the Viking Explorers yacht rally (www.vikingexplorersrally.com) for allowing us to work with their clients to recruit the survey yachts; Dr Jesús Ramón Barriuso Díez (Calplas, Basque Country, Spain) for designing the sampling filter; and the editor and reviewers for their constructive assessment, which materially improved the manuscript.

Financial support

This research received no specific grant from any public, commercial or not-for-profit funding agency. The fieldwork was carried out by volunteer citizen-science crews, and the work was supported by the GOES Foundation.

References

Aeschlimann, M., Li, G., Kanji, Z. A., and Mitrano, D. M.: Potential impacts of atmospheric microplastics and nanoplastics on cloud formation processes, Nat. Geosci., 15, 967–975, https://doi.org/10.1038/s41561-022-01051-9, 2022.

Aiken, J., Rees, N., Hooker, S., Holligan, P., Bale, A., Robins, D., Moore, G., Harris, R., and Pilgrim, D.: The Atlantic Meridional Transect: overview and synthesis of data, Prog. Oceanogr., 45, 257–312, https://doi.org/10.1016/S0079-6611(00)00005-7, 2000.

Allen, S., Allen, D., Phoenix, V. R., Le Roux, G., Jiménez, P. D., Simonneau, A., Binet, S., and Galop, D.: Atmospheric transport and deposition of microplastics in a remote mountain catchment, Nat. Geosci., 12, 339–344, https://doi.org/10.1038/s41561-019-0335-5, 2019.

Asmussen-Schäfer, F., Ribas-Ribas, M., Wurl, O., and Friedrichs, G.: Linking surface coverage with surfactant activity to refine the role of surfactants for air–sea gas exchange, Biogeosciences, 23, 3159–3178, https://doi.org/10.5194/bg-23-3159-2026, 2026.

23

https://doi.org/10.5194/egusphere-2026-3979
Preprint. Discussion started: 29 July 2026

Assis, C. A. M., Pinho, L. Q., Fernandes, A. M., Araujo, M., and Cotrim da Cunha, L.: Reconstruction of the marine carbonate system at the Western Tropical Atlantic: trends and variabilities from 20 years of the PIRATA program, Front. Mar. Sci., 11, 1286960, https://doi.org/10.3389/fmars.2024.1286960, 2024.

Aves, A. R., Revell, L. E., Gaw, S., Ruffell, H., Schuddeboom, A., Wotherspoon, N. E., LaRue, M., and McDonald, A. J.: First evidence of microplastics in Antarctic snow, Cryosphere, 16, 2127–2145, https://doi.org/10.5194/tc-16-2127-2022, 2022.

Bar-On, Y. M., Phillips, R., and Milo, R.: The biomass distribution on Earth, Proc. Natl Acad. Sci. USA, 115, 6506–6511, https://doi.org/10.1073/pnas.1711842115, 2018.

Barbeau, K., Moffett, J. W., Caron, D. A., Croot, P. L., and Erdner, D. L.: Role of protozoan grazing in relieving iron limitation of phytoplankton, Nature, 380, 61–64, https://doi.org/10.1038/380061a0, 1996.

Basterretxea, G., Font-Muñoz, J. S., Hernández-Carrasco, I., and Sañudo-Wilhelmy, S. A.: Global variability of high-nutrient low-chlorophyll regions using neural networks and wavelet coherence analysis, Ocean Sci., 19, 973–990, https://doi.org/10.5194/os-19-973-2023, 2023.

Beaugrand, G., Conversi, A., Atkinson, A., Cloern, J., Chiba, S., Fonda-Umani, S., Kirby, R. R., Greene, C. H., Goberville, E., Otto, S. A., Reid, P. C., Stemmann, L., and Edwards, M.: Prediction of unprecedented biological shifts in the global ocean, Nat. Clim. Change, 9, 237–243, https://doi.org/10.1038/s41558-019-0420-1, 2019.

Bergmann, M., Mützel, S., Primpke, S., Tekman, M. B., Trachsel, J., and Gerdts, G.: White and wonderful? Microplastics prevail in snow from the Alps to the Arctic, Sci. Adv., 5, eaax1157, https://doi.org/10.1126/sciadv.aax1157, 2019.

Bond, T. C., Doherty, S. J., Fahey, D. W., Forster, P. M., Berntsen, T., DeAngelo, B. J., Flanner, M. G., Ghan, S., Kärcher, B., Koch, D., Kinne, S., Kondo, Y., Quinn, P. K., Sarofim, M. C., Schultz, M. G., Schulz, M., Venkataraman, C., Zhang, H., Zhang, S., Bellouin, N., Guttikunda, S. K., Hopke, P. K., Jacobson, M. Z., Kaiser, J. W., Klimont, Z., Lohmann, U., Schwarz, J. P., Shindell, D., Storelvmo, T., Warren, S. G., and Zender, C. S.: Bounding the role of black carbon in the climate system, J. Geophys. Res. Atmos., 118, 5380–5552, https://doi.org/10.1002/jgrd.50171, 2013.

Botterell, Z. L. R., Beaumont, N., Dorrington, T., Steinke, M., Thompson, R. C., and Lindeque, P. K.: Bioavailability and effects of microplastics on marine zooplankton: a review, Environ. Pollut., 245, 98–110, https://doi.org/10.1016/j.envpol.2018.10.065, 2019.

Boyce, D. G., Lewis, M. R., and Worm, B.: Global phytoplankton decline over the past century, Nature, 466, 591–596, https://doi.org/10.1038/nature09268, 2010.

Brahney, J., Mahowald, N., Prank, M., Cornwell, G., Klimont, Z., Matsui, H., and Prather, K. A.: Constraining the atmospheric limb of the plastic cycle, Proc. Natl Acad. Sci. USA, 118, e2020719118, https://doi.org/10.1073/pnas.2020719118, 2021.

Breitburg, D., Levin, L. A., Oschlies, A., Grégoire, M., Chavez, F. P., Conley, D. J., Garçon, V., Gilbert, D., Gutiérrez, D., Isensee, K., Jacinto, G. S., Limburg, K. E., Montes, I., Naqvi, S. W. A., Pitcher, G. C., Rabalais, N. N., Roman, M. R., Rose, K. A., Seibel, B. A., Telszewski, M., Yasuhara, M., and Zhang, J.: Declining oxygen in the global ocean and coastal waters, Science, 359, eaam7240, https://doi.org/10.1126/science.aam7240, 2018.

Cael, B. B., Bisson, K., Boss, E., Dutkiewicz, S., and Henson, S.: Global climate-change trends detected in indicators of ocean ecology, Nature, 619, 551–554, https://doi.org/10.1038/s41586-023-06321-z, 2023.

https://doi.org/10.5194/egusphere-2026-3979
Preprint. Discussion started: 29 July 2026

Cai, W.-J., Hu, X., Huang, W.-J., Murrell, M. C., Lehrter, J. C., Lohrenz, S. E., Chou, W.-C., Zhai, W., Hollibaugh, J. T., Wang, Y., Zhao, P., Guo, X., Gundersen, K., Dai, M., and Gong, G.-C.: Acidification of subsurface coastal waters enhanced by eutrophication, Nat. Geosci., 4, 766–770, https://doi.org/10.1038/ngeo1297, 2011.

Charlson, R. J., Lovelock, J. E., Andreae, M. O., and Warren, S. G.: Oceanic phytoplankton, atmospheric sulphur, cloud albedo and climate, Nature, 326, 655–661, https://doi.org/10.1038/326655a0, 1987.

Chisholm, S. W., Olson, R. J., Zettler, E. R., Goericke, R., Waterbury, J. B., and Welschmeyer, N. A.: A novel free-living prochlorophyte abundant in the oceanic euphotic zone, Nature, 334, 340–343, https://doi.org/10.1038/334340a0, 1988.

Cole, M., Lindeque, P., Fileman, E., Halsband, C., Goodhead, R., Moger, J., and Galloway, T. S.: Microplastic ingestion by zooplankton, Environ. Sci. Technol., 47, 6646–6655, https://doi.org/10.1021/es400663f, 2013.

Cózar, A., Echevarría, F., González-Gordillo, J. I., Irigoien, X., Úbeda, B., Hernández-León, S., Palma, Á. T., Navarro, S., García-de-Lomas, J., Ruiz, A., Fernández-de-Puelles, M. L., and Duarte, C. M.: Plastic debris in the open ocean, Proc. Natl Acad. Sci. USA, 111, 10239–10244, https://doi.org/10.1073/pnas.1314705111, 2014.

Cunliffe, M., Engel, A., Frka, S., Gašparović, B., Guitart, C., Murrell, J. C., Salter, M., Stolle, C., Upstill-Goddard, R., and Wurl, O.: Sea surface microlayers: a unified physicochemical and biological perspective, Prog. Oceanogr., 109, 104–116, https://doi.org/10.1016/j.pocean.2012.08.004, 2013.

Dando, P. R., Hughes, J. A., Leahy, Y., Niven, S. J., Taylor, L. J., and Smith, C.: Gas venting rates from submarine hydrothermal areas around the island of Milos, Hellenic Volcanic Arc, Cont. Shelf Res., 15, 913–929, https://doi.org/10.1016/0278-4343(95)80002-U, 1995.

Davies, T. W. and Smyth, T.: Darkening of the global ocean, Glob. Change Biol., 31, e70227, https://doi.org/10.1111/gcb.70227, 2025.

Desforges, J.-P. W., Galbraith, M., and Ross, P. S.: Ingestion of microplastics by zooplankton in the NE Pacific, Arch. Environ. Contam. Toxicol., 69, 320–330, https://doi.org/10.1007/s00244-015-0172-5, 2015.

Devault, D. A., Pierre, R., Marfaing, H., Dolique, F., and Lopez, P.-J.: Sargassum contamination and consequences for downstream uses: a review, J. Appl. Phycol., 32, 1793–1830, https://doi.org/10.1007/s10811-020-02250-w, 2020.

Dryden, H. and Duncan, D.: GOES North Atlantic transect (2022): per-station particle counts, individual particle sizes, and crew field logs [data set], Zenodo, https://doi.org/10.5281/zenodo.21477682, 2026.

Dutkiewicz, S., Morris, J. J., Follows, M. J., Scott, J., Levitan, O., Dyhrman, S. T., and Berman-Frank, I.: Impact of ocean acidification on the structure of future phytoplankton communities, Nat. Clim. Change, 5, 1002–1006, https://doi.org/10.1038/nclimate2722, 2015.

Engel, A., Bange, H. W., Cunliffe, M., Burrows, S. M., Friedrichs, G., Galgani, L., Herrmann, H., Hertkorn, N., Johnson, M., Liss, P. S., Quinn, P. K., Schartau, M., Soloviev, A., Stolle, C., Upstill-Goddard, R. C., van Pinxteren, M., and Zäncker, B.: The ocean's vital skin: toward an integrated understanding of the sea surface microlayer, Front. Mar. Sci., 4, 165, https://doi.org/10.3389/fmars.2017.00165, 2017.

Engel, A., Friedrichs, G., Krall, K. E., and Jähne, B.: Wind-induced collapse of the biopolymeric surface microlayer induces sudden changes in sea surface roughness, Biogeosciences, 23, 2101–2117, https://doi.org/10.5194/bg-23-2101-2026, 2026.

25

https://doi.org/10.5194/egusphere-2026-3979
Preprint. Discussion started: 29 July 2026

Evans, M. C. and Ruf, C. S.: Toward the detection and imaging of ocean microplastics with a spaceborne radar, IEEE Trans. Geosci. Remote Sens., 60, 4202709, https://doi.org/10.1109/TGRS.2021.3081691, 2022.

Feely, R. A., Sabine, C. L., Hernandez-Ayon, J. M., Ianson, D., and Hales, B.: Evidence for upwelling of corrosive "acidified" water onto the continental shelf, Science, 320, 1490–1492, https://doi.org/10.1126/science.1155676, 2008.

Fernández de Puelles, M. L., Gazá, M., Cabanellas-Reboredo, M., Santandreu, M. del M., Irigoien, X., González-Gordillo, J. I., Duarte, C. M., and Hernández-León, S.: Zooplankton abundance and diversity in the tropical and subtropical ocean, Diversity, 11, 203, https://doi.org/10.3390/d11110203, 2019.

Field, C. B., Behrenfeld, M. J., Randerson, J. T., and Falkowski, P.: Primary production of the biosphere: integrating terrestrial and oceanic components, Science, 281, 237–240, https://doi.org/10.1126/science.281.5374.237, 1998.

Fuller, R., Landrigan, P. J., Balakrishnan, K., Bathan, G., Bose-O'Reilly, S., Brauer, M., Caravanos, J., Chiles, T., Cohen, A., Corra, L., Cropper, M., Ferraro, G., Hanna, J., Hanrahan, D., Hu, H., Hunter, D., Janata, G., Kupka, R., Lanphear, B., Lichtveld, M., Martin, K., Mustapha, A., Sanchez-Triana, E., Sandilya, K., Schaefli, L., Shaw, J., Seddon, J., Suk, W., Téllez-Rojo, M. M., and Yan, C.: Pollution and health: a progress update, Lancet Planet. Health, 6, e535–e547, https://doi.org/10.1016/S2542-5196(22)00090-0, 2022.

Galloway, T. S., Cole, M., and Lewis, C.: Interactions of microplastic debris throughout the marine ecosystem, Nat. Ecol. Evol., 1, 0116, https://doi.org/10.1038/s41559-017-0116, 2017.

Garrett, W. D.: The organic chemical composition of the ocean surface, Deep-Sea Res., 14, 221–227, https://doi.org/10.1016/0011-7471(67)90007-1, 1967.

Gimeno, L., Stohl, A., Trigo, R. M., Dominguez, F., Yoshimura, K., Yu, L., Drumond, A., Durán-Quesada, A. M., and Nieto, R.: Oceanic and terrestrial sources of continental precipitation, Rev. Geophys., 50, RG4003, https://doi.org/10.1029/2012RG000389, 2012.

Gledhill, D. K., Wanninkhof, R., Millero, F. J., and Eakin, M.: Ocean acidification of the Greater Caribbean Region 1996–2006, J. Geophys. Res. Oceans, 113, C10031, https://doi.org/10.1029/2007JC004629, 2008.

González-Alemán, J. J., Insua-Costa, D., Bazile, E., González-Herrero, S., Miglietta, M. M., Groenemeijer, P., and Donat, M. G.: Anthropogenic warming had a crucial role in triggering the historic and destructive Mediterranean derecho in summer 2022, Bull. Am. Meteorol. Soc., 104, https://doi.org/10.1175/BAMS-D-23-0119.1, 2023.

González-Dávila, M. and Santana-Casiano, J. M.: Long-term trends of pH and inorganic carbon in the Eastern North Atlantic: the ESTOC site, Front. Mar. Sci., 10, 1236214, https://doi.org/10.3389/fmars.2023.1236214, 2023.

Hassoun, A. E. R., Gemayel, E., Krasakopoulou, E., Goyet, C., Abboud-Abi Saab, M., Guglielmi, V., Touratier, F., and Falco, C.: Acidification of the Mediterranean Sea from anthropogenic carbon penetration, Deep-Sea Res. I, 102, 1–15, https://doi.org/10.1016/j.dsr.2015.04.005, 2015.

Held, I. M. and Soden, B. J.: Water vapor feedback and global warming, Annu. Rev. Energy Environ., 25, 441–475, https://doi.org/10.1146/annurev.energy.25.1.441, 2000.

Hönisch, B., Ridgwell, A., Schmidt, D. N., Thomas, E., Gibbs, S. J., Sluijs, A., Zeebe, R., Kump, L., Martindale, R. C., Greene, S. E., Kiessling, W., Ries, J., Zachos, J. C., Royer, D. L., Barker, S., Marchitto, T. M., Moyer, R., Pelejero, C., Ziveri, P., Foster,

26

https://doi.org/10.5194/egusphere-2026-3979
Preprint. Discussion started: 29 July 2026

G. L., and Williams, B.: The geological record of ocean acidification, Science, 335, 1058–1063, https://doi.org/10.1126/science.1208277, 2012.

IPBES: Global Assessment Report on Biodiversity and Ecosystem Services of the Intergovernmental Science-Policy Platform on Biodiversity and Ecosystem Services, IPBES Secretariat, Bonn, 2019.

Jamal, C., Makaoui, A., Chierici, M., Cervantes, D., Chair, A., Nait Hammou, H., Idrissi, M., Bouthir, F. Z., Ettahiri, O., Yousfi, S., and Bouamrani, M. L.: Seasonal upwelling drives surface water biogeochemistry with implication for ocean acidification along the Northwest African coast, Front. Mar. Sci., 12, 1579941, https://doi.org/10.3389/fmars.2025.1579941, 2025.

Jiang, L.-Q., Carter, B. R., Feely, R. A., Lauvset, S. K., and Olsen, A.: Surface ocean pH and buffer capacity, Sci. Rep., 9, 18624, https://doi.org/10.1038/s41598-019-55039-4, 2019.

Kroeker, K. J., Kordas, R. L., Crim, R., Hendriks, I. E., Ramajo, L., Singh, G. S., Duarte, C. M., and Gattuso, J.-P.: Impacts of ocean acidification on marine organisms: quantifying sensitivities and interaction with warming, Glob. Change Biol., 19, 1884–1896, https://doi.org/10.1111/gcb.12179, 2013.

Kvale, K., Prowe, A. E. F., Chien, C. T., Landolfi, A., and Oschlies, A.: Zooplankton grazing of microplastic can accelerate global loss of ocean oxygen, Nat. Commun., 12, 2358, https://doi.org/10.1038/s41467-021-22554-w, 2021.

Landrigan, P. J., Stegeman, J. J., Fleming, L. E., Allemand, D., Anderson, D. M., Backer, L. C., Brucker-Davis, F., Chevalier, N., Corra, L., Czerucka, D., Bottein, M.-Y. D., Demeneix, B., Depledge, M., Deheyn, D. D., Dorman, C. J., Fénichel, P., Fisher, S., Gaill, F., Galgani, F., Gaze, W. H., Giuliano, L., Grandjean, P., Hahn, M. E., Hamdoun, A., Hess, P., Judson, B., Laborde, A., McGlade, J., Mu, J., Mustapha, A., Neira, M., Noble, R. T., Pedrotti, M. L., Reddy, C., Rocklöv, J., Scharler, U. M., Shanmugam, H., Taghian, G., van de Water, J. A. J. M., Vezzulli, L., Weihe, P., Zeka, A., Raps, H., and Rampal, P.: Human health and ocean pollution, Ann. Glob. Health, 86, 151, https://doi.org/10.5334/aogh.2831, 2020.

Lapointe, B. E., Brewton, R. A., Herren, L. W., Wang, M., Hu, C., McGillicuddy, D. J., Lindell, S., Hernandez, F. J., and Morton, P. L.: Nutrient content and stoichiometry of pelagic Sargassum reflects increasing nitrogen availability in the Atlantic Basin, Nat. Commun., 12, 3060, https://doi.org/10.1038/s41467-021-23135-7, 2021.

Laws, E. A.: Evaluation of in situ phytoplankton growth rates, Annu. Rev. Mar. Sci., 5, 247–268, https://doi.org/10.1146/annurev-marine-121211-172258, 2013.

Lee, W.-K., Sim, Y., Ju, S.-J., Kim, D., Jeong, J., and Kim, S.-J.: Oceanic determinants of microplastic bioaccumulation in fauna of deep-sea hydrothermal vents: comparative study of the southwestern Pacific and Indian Oceans, Water Res., https://doi.org/10.1016/j.watres.2026.126245, 2026.

López-Puertas, A., Wurl, O., Frka, S., and Ribas-Ribas, M.: Diel variability affects the inorganic carbon system in the sea-surface microlayer and influences air–sea CO_2 flux estimates, Ocean Sci., 21, 3471–3485, https://doi.org/10.5194/os-21-3471-2025, 2025.

Ma, H., Pu, S., Liu, S., Bai, Y., Mandal, S., and Xing, B.: Microplastics in aquatic environments: toxicity to trigger ecological consequences, Environ. Pollut., 261, 114089, https://doi.org/10.1016/j.envpol.2020.114089, 2020.

Mai, L., Sun, X.-F., Xia, L.-L., Bao, L.-J., Liu, L.-Y., and Zeng, E. Y.: Global riverine plastic outflows, Environ. Sci. Technol., 54, 10049–10056, https://doi.org/10.1021/acs.est.0c02273, 2020.

27

https://doi.org/10.5194/egusphere-2026-3979
Preprint. Discussion started: 29 July 2026

Mato, Y., Isobe, T., Takada, H., Kanehiro, H., Ohtake, C., and Kaminuma, T.: Plastic resin pellets as a transport medium for toxic chemicals in the marine environment, Environ. Sci. Technol., 35, 318–324, https://doi.org/10.1021/es0010498, 2001.

McGillicuddy, D. J., Morton, P. L., Brewton, R. A., Hu, C., Kelly, T. B., Solow, A. R., and Lapointe, B. E.: Nutrient and arsenic biogeochemistry of Sargassum in the western Atlantic, Nat. Commun., 14, 6205, https://doi.org/10.1038/s41467-023-41904-4, 2023.

McQuatters-Gollop, A., Holland, M. M., Artigas, L. F., Louchart, A. P., Atkinson, A., Aubert, A., Best, M., Blauw, A., Bresnan, E., Devlin, M., Enserink, L., Faith, M. P., Goberville, E., Heyden, B., Jakobsen, H. H., Johansen, M., Johns, D. G., Ostle, C., Rombouts, I., Schilder, J., Tett, P., and Vincent, D.: Integrating plankton indicators to assess the state of pelagic habitats in the Northeast Atlantic, Ecol. Indic., 174, 115005, https://doi.org/10.1016/j.ecolind.2026.115005, 2026.

Murphy, E. L., Baechler, B. R., Roman, L., Leonard, G. H., Mallos, N. J., Santos, R. G., and Rochman, C. M.: A quantitative risk assessment framework for mortality due to macroplastic ingestion in seabirds, marine mammals, and sea turtles, Proc. Natl Acad. Sci. USA, 122, e2415492122, https://doi.org/10.1073/pnas.2415492122, 2025.

Mustaffa, N. I. H., Ribas-Ribas, M., Banko-Kubis, H. M., and Wurl, O.: Global reduction of in situ CO_2 transfer velocity by natural surfactants in the sea-surface microlayer, Proc. R. Soc. A, 476, 20190763, https://doi.org/10.1098/rspa.2019.0763, 2020.

O'Dowd, C. D., Smith, M. H., Consterdine, I. E., and Lowe, J. A.: Marine aerosol, sea-salt and the marine sulphur cycle, Atmos. Environ., 31, 73–80, https://doi.org/10.1016/S1352-2310(96)00106-9, 1997.

O'Dowd, C. D., Facchini, M. C., Cavalli, F., Ceburnis, D., Mircea, M., Decesari, S., Fuzzi, S., Yoon, Y. J., and Putaud, J.-P.: Biogenically driven organic contribution to marine aerosol, Nature, 431, 676–680, https://doi.org/10.1038/nature02959, 2004.

Pabortsava, K. and Lampitt, R. S.: High concentrations of plastic hidden beneath the surface of the Atlantic Ocean, Nat. Commun., 11, 4073, https://doi.org/10.1038/s41467-020-17932-9, 2020.

Parrella, F., Brizzolara, S., Holzner, M., and Mitrano, D. M.: Impact of heteroaggregation between microplastics and algae on particle vertical transport, Nat. Water, 2, 541–552, https://doi.org/10.1038/s44221-024-00248-z, 2024.

Pereira, R., Ashton, I., Sabbaghzadeh, B., Shutler, J. D., and Upstill-Goddard, R. C.: Reduced air–sea CO_2 exchange in the Atlantic Ocean due to biological surfactants, Nat. Geosci., 11, 492–496, https://doi.org/10.1038/s41561-018-0136-2, 2018.

Polovina, J. J., Howell, E. A., and Abecassis, M.: Ocean's least productive waters are expanding, Geophys. Res. Lett., 35, L03618, https://doi.org/10.1029/2007GL031745, 2008.

Quinn, P. K. and Bates, T. S.: The case against climate regulation via oceanic phytoplankton sulphur emissions, Nature, 480, 51–56, https://doi.org/10.1038/nature10580, 2011.

Riebesell, U., Zondervan, I., Rost, B., Tortell, P. D., Zeebe, R. E., and Morel, F. M. M.: Reduced calcification of marine plankton in response to increased atmospheric CO_2, Nature, 407, 364–367, https://doi.org/10.1038/35030078, 2000.

Rodríguez-Martínez, R. E., Roy, P. D., Torrescano-Valle, N., Cabanillas-Terán, N., Carrillo-Domínguez, S., Collado-Vides, L., García-Sánchez, M., and van Tussenbroek, B. I.: Element concentrations in pelagic Sargassum along the Mexican Caribbean coast in 2018–2019, PeerJ, 8, e8667, https://doi.org/10.7717/peerj.8667, 2020.

Shen, M., Ye, S., Zeng, G., Zhang, Y., Xing, L., Tang, W., Wen, X., and Liu, S.: Can microplastics pose a threat to ocean carbon sequestration?, Mar. Pollut. Bull., 150, 110712, https://doi.org/10.1016/j.marpolbul.2019.110712, 2020.

https://doi.org/10.5194/egusphere-2026-3979
Preprint. Discussion started: 29 July 2026

807 Silva, A., Nikzad, S., Barthelmeß, T., Engel, A., Herrmann, H., van Pinxteren, M., Wirtz, K., Wurl, O., and Schartau, M.: Meta-
808 analytical insights into organic matter enrichment in the surface microlayer, Biogeosciences, 23, 1697–1718,
809 https://doi.org/10.5194/bg-23-1697-2026, 2026.
810 Tetu, S. G., Sarker, I., Schrameyer, V., Pickford, R., Elbourne, L. D. H., Moore, L. R., and Paulsen, I. T.: Plastic leachates impair
811 growth and oxygen production in Prochlorococcus, Commun. Biol., 2, 184, https://doi.org/10.1038/s42003-019-0410-x, 2019.
812 Trainic, M., Flores, J. M., Pinkas, I., Pedrotti, M. L., Lombard, F., Bourdin, G., Gorsky, G., Boss, E., Rudich, Y., Vardi, A., and
813 Koren, I.: Airborne microplastic particles detected in the remote marine atmosphere, Commun. Earth Environ., 1, 64,
814 https://doi.org/10.1038/s43247-020-00061-y, 2020.
815 Trick, C. G., Bill, B. D., Cochlan, W. P., Wells, M. L., Trainer, V. L., and Pickell, L. D.: Iron enrichment stimulates toxic diatom
816 production in high-nitrate, low-chlorophyll areas, Proc. Natl Acad. Sci. USA, 107, 5887–5892,
817 https://doi.org/10.1073/pnas.0910579107, 2010.
818 Tyrrell, T., Merico, A., Waniek, J. J., Wong, C. S., Metzl, N., and Whitney, F.: Effect of seafloor depth on phytoplankton blooms in
819 HNLC regions, J. Geophys. Res. Biogeosci., 110, G02007, https://doi.org/10.1029/2005JG000041, 2005.
820 Vereshchaka, A. L., Abyzova, G., Lunina, A., and Musaeva, E.: The deep-sea zooplankton of the North, Central, and South
821 Atlantic: Biomass, abundance, diversity, Deep-Sea Res. II, 137, 89–101, https://doi.org/10.1016/j.dsr2.2016.06.017, 2017.
822 Wang, M., Hu, C., Barnes, B. B., Mitchum, G., Lapointe, B., and Montoya, J. P.: The great Atlantic Sargassum belt, Science, 365,
823 83–87, https://doi.org/10.1126/science.aaw7912, 2019.
824 Williams, P. M., Carlucci, A. F., Henrichs, S. M., Van Vleet, E. S., Horrigan, S. G., Reid, F. M. H., and Robertson, K. J.: Chemical
825 and microbiological studies of sea-surface films, Mar. Chem., 19, 17–98, https://doi.org/10.1016/0304-4203(86)90033-2,
826 1986.
827 Woodd-Walker, R. S., Ward, P., and Clarke, A.: Large-scale patterns in surface zooplankton across a 20°W meridional transect of
828 the NE Atlantic, Deep-Sea Res. II, 47, 2903–2924, https://doi.org/10.1016/S0967-0645(00)00114-4, 2000.
829 Wurl, O. and Obbard, J. P.: A review of pollutants in the sea-surface microlayer (SML), Mar. Pollut. Bull., 48, 1016–1030,
830 https://doi.org/10.1016/j.marpolbul.2004.03.016, 2004.
831 WWAP (UNESCO World Water Assessment Programme): The United Nations World Water Development Report 2017:
832 Wastewater, the Untapped Resource, UNESCO, Paris, 2017.
833 Yoon, J.-E., Yoo, K.-C., Macdonald, A. M., Yoon, H.-I., Park, K.-T., Yang, E. J., Kim, H.-C., Lee, J. I., Lee, M. K., Jung, J., Park, J.,
834 Lee, J., Kim, S., Kim, S.-S., Kim, K., and Kim, I.-N.: Reviews and syntheses: ocean iron fertilization experiments — past,
835 present, and future looking to a future Korean Iron Fertilization Experiment in the Southern Ocean (KIFES) project,
836 Biogeosciences, 15, 5847–5889, https://doi.org/10.5194/bg-15-5847-2018, 2018.
837 You, Y., Ting, M., and Biasutti, M.: Climate warming contributes to the record-shattering 2022 Pakistan rainfall, npj Clim. Atmos.
838 Sci., 7, 89, https://doi.org/10.1038/s41612-024-00630-4, 2024.
839 Zhang, Z., Cai, W., Liu, L., Liu, C., and Chen, F.: Direct determination of thickness of the sea-surface microlayer, Sci. China Ser. B,
840 46, 339–351, https://doi.org/10.1360/02yb0192, 2003.

https://doi.org/10.5194/egusphere-2026-3979
Preprint. Discussion started: 29 July 2026

841 Zhu, R., Zhang, Z., Zhang, N., Zhong, H., Zhou, F., Zhang, X., Liu, C., Huang, Y., Yuan, Y., Wang, Y., Li, C., Shi, H., Rillig, M. C.,
842 Dang, F., Ren, H., Zhang, Y., and Xing, B.: A global estimate of multiecosystem photosynthesis losses under microplastic
843 pollution, Proc. Natl Acad. Sci. USA, 122, e2423957122, https://doi.org/10.1073/pnas.2423957122, 2025.
844 Ziccardi, L., Edgington, A., Hentz, K., Kulacki, K., and Driscoll, S.: Microplastics as vectors for bioaccumulation of hydrophobic
845 organic chemicals, Environ. Toxicol. Chem., 35, 1667–1676, https://doi.org/10.1002/etc.3461, 2016.

30